Robotics and Autonomous Systems 58 (2010) 16–26

Contents lists available at ScienceDirect

Robotics and Autonomous Systems

journal homepage: www.elsevier.com/locate/robot

An adaptive fuzzy sliding mode controller for remotely operated underwater vehicles

Wallace M. Bessa [a,*], Max S. Dutra [b], Edwin Kreuzer [c]

[a] UFRN, Federal University of Rio Grande do Norte, Centro de Tecnologia, Departamento de Engenharia Mecânica, Campus Universitário Lagoa Nova, CEP 59072-970, Natal, RN, Brazil

[b] COPPE/UFRJ, Federal University of Rio de Janeiro, P.O. Box 68.503, CEP 21945-970, Rio de Janeiro, Brazil

[c] TUHH, Hamburg University of Technology, Eissendorfer Strasse 42, D-21071, Hamburg, Germany

ARTICLE INFO

Article history:
Received 29 June 2008
Received in revised form
23 July 2009
Accepted 2 September 2009
Available online 10 September 2009

Keywords:
Adaptive algorithms
Dynamic positioning
Fuzzy logic
Sliding modes
Remotely operated underwater vehicles

ABSTRACT

Sliding mode control is a very attractive control scheme because of its robustness against both structured and unstructured uncertainties as well as external disturbances. In this way, it has been widely employed for the dynamic positioning of remotely operated underwater vehicles. Nevertheless, in such situations the discontinuities in the control law must be smoothed out to avoid the undesirable chattering effects. The adoption of properly designed boundary layers has proven effective in completely eliminating chattering, however, leading to an inferior tracking performance. This work describes the development of a dynamic positioning system for remotely operated underwater vehicles. The adopted approach is primarily based on the sliding mode control strategy and enhanced by an adaptive fuzzy algorithm for uncertainty/disturbance compensation. Using the Lyapunov stability theory and Barbalat's lemma, the boundedness and convergence properties of the closed-loop signals are analytically proven. The performance of the proposed control scheme is also evaluated by means of numerical simulations.

1. Introduction

The control system is one of the most important elements of an underwater robotic vehicle, and its characteristics (advantages and disadvantages) play an essential role when one has to choose a vehicle for a specific mission. Unfortunately, the problem of designing accurate positioning systems for underwater robotic vehicles still challenges many engineers and researchers interested in this particular branch of engineering science. A growing number of papers dedicated to the position and orientation control of such vehicles confirm the necessity of the development of a controller, that could deal with the inherent nonlinear system dynamics, imprecise hydrodynamic coefficients, and external disturbances.

It has already been shown [1,2] that, in the case of underwater vehicles, the traditional control methodologies are not the most suitable choice and cannot guarantee the required tracking performance. On the other hand, sliding mode control, due to its robustness against modeling inaccuracies and external disturbance, has proven to be a very attractive approach to cope with these problems [3–12]. But a well known drawback of conventional sliding mode controllers is the chattering effect. To overcome the undesired effects of the control chattering, Slotine [13] proposed the adoption of a thin boundary layer neighboring the switching surface, by replacing the sign function by a saturation function. This substitution can minimize or, when desired, even completely eliminate chattering, but turns *perfect tracking* into a *tracking with guaranteed precision* problem, which in fact means that a steady-state error will always remain. In order to enhance the tracking performance inside the boundary layer, some adaptive strategy should be used for uncertainty/disturbance compensation.

Due to the possibility of expressing human experience in an algorithmic manner, fuzzy logic has been largely employed in the past few decades to both control and identification of dynamical systems. In spite of the simplicity of this heuristic approach, in some situations a more rigorous mathematical treatment of the problem is required. Recently, much effort has been made to combine fuzzy logic with nonlinear control methodology. In [14] a globally stable adaptive fuzzy controller was proposed using the Lyapunov stability theory to develop the adaptive law. Combining fuzzy logic with sliding mode control, Palm [15] used the switching variable s to define a fuzzy boundary layer. Some improvements to this control scheme appeared in [16,17]. Wong et al. [18] proposed a fuzzy logic controller which combines a sliding mode controller and a proportional plus integral controller. A sliding mode controller that incorporates a fuzzy tuning technique was analyzed in [19]. By defining a generalized error transformation as

* Corresponding author. Tel.: +55 84 3215 3740; fax: +55 84 3215 3740.
E-mail addresses: wmbessa@ufrnet.br (W.M. Bessa), max@mecanica.ufrj.br (M.S. Dutra), kreuzer@tu-harburg.de (E. Kreuzer).

0921-8890/$ – see front matter © 2009 Elsevier B.V. All rights reserved.
doi:10.1016/j.robot.2009.09.001

a complement to the conventional switching variable, Liang and Su [20] developed a stable fuzzy sliding mode control scheme. Cheng and Chien [21] proposed an adaptive sliding mode controller based on T–S fuzzy models and Wu and Juang [22] showed that fuzzy sliding surfaces can be established by solving a set of linear matrix inequalities.

A robust and very attractive approach was proposed in [23]. Yoo and Ham [23] used fuzzy inference systems to approximate the unknown system dynamics within the sliding mode controller. Some improvements to this methodology are suggested in [24–28] and an application to an underwater vehicle is presented in [5]. A drawback of this approach is the adoption of the state variables in the premise of the fuzzy rules. For higher-order systems the number of fuzzy sets and fuzzy rules becomes incredibly large, which compromises the applicability of this technique.

In order to reduce the number of fuzzy sets and rules and consequently simplify the design process, Bessa and Barrêto [29] proposed the adoption of the switching variable s, instead of the state variables, in the premise of the fuzzy rules. This control strategy has already been successfully applied to the depth regulation of remotely operated underwater vehicles [3] and to chaos control in a nonlinear pendulum [30].

In this work, the control scheme presented in [29] is employed for the dynamic positioning of underwater vehicles with four controllable degrees of freedom. The adoption of a reduced order mathematical model and the development of the control system in a decentralized fashion, neglecting cross-coupling terms, is discussed. Rigorous proofs of the boundedness and convergence properties of the closed-loop signals by means of Lyapunov stability theory and Barbalat's lemma are presented. This analytical result proves that the convergence region of the tracking error vector is even smaller than that shown in [3]. Numerical results are also provided to confirm the control system efficacy.

2. Vehicle dynamics model

A reasonable model to describe the underwater vehicle's dynamical behavior must include the rigid-body dynamics of the vehicle's body and a representation of the surrounding fluid dynamics. Such a model must be composed of a system of ordinary differential equations, to represent rigid-body dynamics, and partial differential equations to represent both tether and fluid dynamics.

In order to overcome the computational problem of solving a system with this degree of complexity, in the majority of publications [3,31–35,12] a lumped parameters approach is employed to approximate vehicle's dynamical behavior.

The equations of motion for underwater vehicles can be presented with respect to an inertial reference frame or with respect to a body-fixed reference frame, Fig. 1. On this basis, the equations of motion for underwater vehicles can be expressed, with respect to the body-fixed reference frame, in the following vectorial form:

$$\mathbf{M}\dot{\boldsymbol{\nu}} + \mathbf{k}(\boldsymbol{\nu}) + \mathbf{h}(\boldsymbol{\nu}) + \mathbf{g}(\mathbf{x}) + \mathbf{p} = \boldsymbol{\tau} \quad (1)$$

where $\boldsymbol{\nu} = [\upsilon_x, \upsilon_y, \upsilon_z, \omega_x, \omega_y, \omega_z]$ is the vector of linear and angular velocities in the body-fixed reference frame, $\mathbf{x} = [x, y, z, \alpha, \beta, \gamma]$ represents the position and orientation with respect to the inertial reference frame, $\mathbf{M}$ is the inertia matrix, which accounts not only for the rigid-body inertia but also for the so-called hydrodynamic added inertia, $\mathbf{k}(\boldsymbol{\nu})$ is the vector of generalized Coriolis and centrifugal forces, $\mathbf{h}(\boldsymbol{\nu})$ represents the hydrodynamic quadratic damping, $\mathbf{g}(\mathbf{x})$ is the vector of generalized restoring forces (gravity and buoyancy), $\mathbf{p}$ stands for occasional disturbances, and $\boldsymbol{\tau}$ is the vector of control forces and moments.

It should be noted that in the case of remotely operated underwater vehicles (ROVs), the metacentric height is sufficiently large

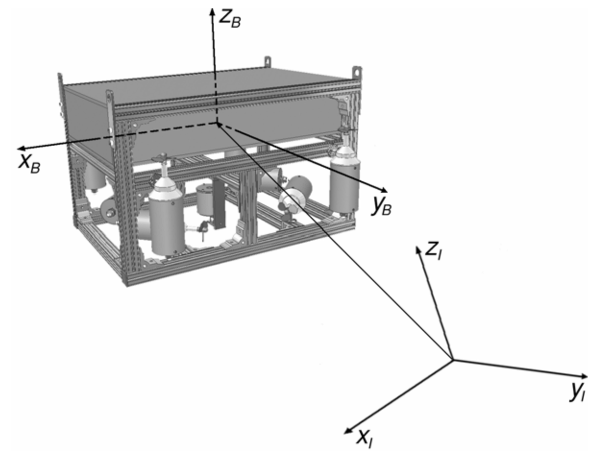

Fig. 1. Underwater vehicle with both inertial and body-fixed reference frames.

to provide the self-stabilization of roll (α) and pitch (β) angles. This particular constructive aspect also allows the order of the dynamic model to be reduced to four degrees of freedom, $\mathbf{x} = [x, y, z, \gamma]$, and the vertical motion (heave) to be decoupled from the motion in the horizontal plane. This simplification can be found in the majority of works presented in the specialized literature [32,36,8,34,35,37,38,12]. Thus, the positioning system of a ROV can be divided in two different parts: Depth control (concerning variable z), and control in the horizontal plane (variables x, y and γ).

Another important issue in the case of ROVs is the disturbance force caused by the umbilical (or tether cable). The umbilical can be treated as a continuum, discretized with the finite element method or modeled as multibody system [39,37]. However, the adoption of any of these approaches requires a computational effort that would be prohibitive for on-line estimation of the control action. A common way to surmount this limitation is to consider the forces and moments exerted by the tether as random, and incorporate them into the vector $\mathbf{p}$.

On this basis, considering that the restoring forces can be passively compensated [35], the most relevant hydrodynamic forces and moments acting on ROVs, as well as the effects produced by the thruster system, are discussed in the following subsections.

2.1. Hydrodynamic forces

Remotely operated underwater vehicles typically operate with velocities never exceeding 2 m/s. Consequently, the hydrodynamic forces (F_h) can be approximated using the *Morison equation* [40]:

$$F_h = \frac{1}{2}C_D A\rho\upsilon|\upsilon| + C_M\rho\nabla\dot{\upsilon} + \rho\nabla\dot{\upsilon}_w \quad (2)$$

where υ and $\dot{\upsilon}$ are, respectively, the relative velocity and the relative acceleration between rigid-body and fluid, $\dot{\upsilon}_w$ is the acceleration of underwater currents, A is a reference area, ρ is the fluid density, ∇ is the fluid's displaced volume, C_D and C_M are coefficients that must be obtained experimentally.

The last term of Eq. (2) is the so-called *Froude–Kriloff force* and will not be considered in this work due the fact, that at normal working depths, the acceleration of the underwater currents is negligible. In this way, the coefficient $C_M\rho\nabla$ of the second term will be called hydrodynamic added mass. The first term represents the nonlinear hydrodynamic quadratic damping. Experimental tests [41] show that Morison equation describes with sufficient accuracy the hydrodynamic effects due to the relative motion between rigid-bodies and water.

2.1.1. Quadratic damping

The effects of the hydrodynamic damping $\mathbf{h}(\boldsymbol{\nu})$ over the vehicle, due not only to the translational but also to rotational motions, can be described in the body-fixed reference frame by:

$$\mathbf{h}(\boldsymbol{\nu}) = \frac{1}{2}\rho[C_{D_x}\upsilon_x|\upsilon_x|, C_{D_y}\upsilon_y|\upsilon_y|, C_{D_z}\upsilon_z|\upsilon_z|, C_{D_\gamma}\omega_z|\omega_z|] \tag{3}$$

where the parameters C_{D_x}, C_{D_y}, C_{D_z} and C_{D_γ} depend on the geometry of the vehicle and should be obtained experimentally in a wind tunnel [37], or on-line estimated with adaptive algorithms in a water tank [42].

2.1.2. Added inertia

Considering that an underwater vehicle typically operates at low speeds, the added inertia matrix, $\mathbf{M}_A \in \mathbb{R}^{4\times4}$, could be assumed as diagonally dominant and described as follows:

$$\mathbf{M}_A = \text{diag}\{C_{M_x}\rho\nabla, C_{M_y}\rho\nabla, C_{M_z}\rho\nabla, C_{M_\gamma}\rho\nabla\}. \tag{4}$$

As with the computation of the hydrodynamic damping, the coefficients C_{M_x}, C_{M_y}, C_{M_z} and C_{M_γ} should be determined experimentally. The matrix $\mathbf{M}_A$ must be combined with the rigid-body inertia matrix in order to obtain the matrix $\mathbf{M}$ of Eq. (1).

2.2. Thruster forces

The steady-state axial thrust F_p produced by marine thrusters is presented in the literature as proportional to the square of propeller's angular velocity Ω [40]. This quadratic relationship can be conveniently represented by

$$F_p = C_T\Omega|\Omega| \tag{5}$$

where C_T is a function of the advance ratio and depends on constructive characteristics of each thruster.

Furthermore, the effect on the vehicle of the force produced by everyone of the N thrusters can be described in body-fixed reference frame by

$$\boldsymbol{\tau} = \mathbf{B}\mathbf{F_p} \tag{6}$$

where $\mathbf{F_p} \in \mathbb{R}^N$ is a vector containing the force produced by each thruster and $\mathbf{B} \in \mathbb{R}^{4\times N}$ is a matrix which represents the distribution of the thrust forces on the vehicle.

Dynamic and more sophisticated thruster models can be found in [43,44].

3. Dynamic positioning system

The dynamic positioning of underwater robotic vehicles is essentially a multivariable control problem. Nevertheless, as demonstrated by Slotine [45], the variable structure control methodology allows different controllers to be separately designed for each degree of freedom (DOF). Over the past decades, decentralized control strategies have been successfully applied to the dynamic positioning of underwater vehicles [5,6,33,35,38,12].

Considering that the control law for each degree of freedom can be easily designed with respect to the inertial reference frame, Eq. (1) should be rewritten in this coordinate system.

Remembering that

$$\dot{\mathbf{x}} = \mathbf{J}(\mathbf{x})\boldsymbol{\nu} \tag{7}$$

where $\mathbf{J}(\mathbf{x})$ is the Jacobian transformation matrix, it can be directly implied that

$$\boldsymbol{\nu} = \mathbf{J}^{-1}(\mathbf{x})\dot{\mathbf{x}} \tag{8}$$

and

$$\dot{\boldsymbol{\nu}} = \dot{\mathbf{J}}^{-1}\dot{\mathbf{x}} + \mathbf{J}^{-1}\ddot{\mathbf{x}}. \tag{9}$$

Therefore, the equations of motion of an underwater vehicle, with respect to the inertial reference frame, becomes

$$\bar{\mathbf{M}}\ddot{\mathbf{x}} + \bar{\mathbf{k}} + \bar{\mathbf{h}} + \bar{\mathbf{p}} = \bar{\boldsymbol{\tau}} \tag{10}$$

where $\bar{\mathbf{M}} = \mathbf{J}^{-\mathrm{T}}\mathbf{M}\mathbf{J}^{-1}$, $\bar{\mathbf{k}} = \mathbf{J}^{-\mathrm{T}}\mathbf{k} + \mathbf{J}^{-\mathrm{T}}\mathbf{M}\dot{\mathbf{J}}^{-1}\dot{\mathbf{x}}$, $\bar{\mathbf{h}} = \mathbf{J}^{-\mathrm{T}}\mathbf{h}$, $\bar{\mathbf{p}} = \mathbf{J}^{-\mathrm{T}}\mathbf{p}$ and $\bar{\boldsymbol{\tau}} = \mathbf{J}^{-\mathrm{T}}\boldsymbol{\tau}$.

In order to develop the control law with a decentralized approach, Eq. (10) can be rewritten as follows:

$$\ddot{x}_i = \bar{m}_i^{-1}(\bar{\tau}_i - \bar{k}_i - \bar{h}_i - \bar{p}_i); \quad i = 1, 2, 3, 4, \tag{11}$$

where x_i, $\bar{\tau}_i$, $\bar{k}_i$, $\bar{h}_i$ and $\bar{p}_i$ are the components of $\mathbf{x} = [x, y, z, \gamma]$, $\bar{\boldsymbol{\tau}}$, $\bar{\mathbf{k}}$, $\bar{\mathbf{h}}$ and $\bar{\mathbf{p}}$, respectively. Concerning $\bar{m}_i$, it represents the main diagonal terms of $\mathbf{J}^{-\mathrm{T}}\mathbf{M}\mathbf{J}^{-1}$. The off-diagonal terms of $\mathbf{J}^{-\mathrm{T}}\mathbf{M}\mathbf{J}^{-1}$ are incorporated in the vector $\bar{\mathbf{p}}$.

Now, let $S_i(t)$ be a sliding surface defined in the state space of each degree of freedom (x_i) by the equation $s_i(\tilde{x}_i, \dot{\tilde{x}}_i) = 0$, with $s_i : \mathbb{R}^2 \to \mathbb{R}$ satisfying

$$s_i(\tilde{x}_i, \dot{\tilde{x}}_i) = \dot{\tilde{x}}_i + \lambda_i\tilde{x}_i \tag{12}$$

where $\tilde{x}_i = x_i - x_{d_i}$ is the tracking error associated to each DOF, $\dot{\tilde{x}}_i$ is the time derivative of $\tilde{x}_i$, x_{d_i} is the correspondent desired trajectory and λ_i are strictly positive constants.

Thus, given the main characteristics of the system to be controlled, the dynamic positioning is done assuming a sliding mode based approach, defining a control law composed by an equivalent control $\hat{\bar{\tau}}_i = \hat{\bar{k}}_i + \hat{\bar{h}}_i + \hat{\bar{p}}_i + \hat{\bar{m}}_i\left(\ddot{x}_{d_i} - \lambda_i\dot{\tilde{x}}_i\right)$ and a discontinuous term $-K_i\,\text{sgn}(s_i)$:

$$\bar{\tau}_i = \hat{\bar{k}}_i + \hat{\bar{h}}_i + \hat{\bar{p}}_i + \hat{\bar{m}}_i\left(\ddot{x}_{d_i} - \lambda_i\dot{\tilde{x}}_i\right) - K_i\,\text{sgn}(s_i) \tag{13}$$

where $\hat{\bar{m}}_i$, $\hat{\bar{k}}_i$, $\hat{\bar{h}}_i$ and $\hat{\bar{p}}_i$ stands for estimates of $\bar{m}_i$, $\bar{k}_i$, $\bar{h}_i$ and $\bar{p}_i$, respectively, and $\text{sgn}(\cdot)$ is defined as:

$$\text{sgn}(s_i) = \begin{cases} -1 & \text{if } s_i < 0 \\ 0 & \text{if } s_i = 0 \\ 1 & \text{if } s_i > 0. \end{cases} \tag{14}$$

Now, given the required control force $\bar{\boldsymbol{\tau}}$ and the thruster's arrangement on the vehicle, the force that should be produced by every thruster can be determined by

$$\mathbf{F}_p = \mathbf{B}^{\mathrm{T}}(\mathbf{B}\mathbf{B}^{\mathrm{T}})^{-1}\mathbf{J}^{-1}\bar{\boldsymbol{\tau}}$$

where $\mathbf{B}^{\mathrm{T}}(\mathbf{B}\mathbf{B}^{\mathrm{T}})^{-1}$ is the pseudo-inverse of matrix $\mathbf{B}$.

In this way, considering the required thrust forces and Eq. (5), the related angular velocity could be easily estimated for each propeller.

It should be emphasized that the lumped parameters approach, adopted to describe the hydrodynamic effects (quadratic damping and added inertia), represents a simplification, and hence only estimates of the actual phenomena are available. Due to the presence of the term $\mathbf{J}^{-\mathrm{T}}\mathbf{M}\dot{\mathbf{J}}^{-1}\dot{\mathbf{x}}$, the vector $\bar{\mathbf{k}}$ cannot be exactly known.

On this basis, the following assumptions must be made:

Assumption 1. The states x_i and $\dot{x}_i$ are available.

Assumption 2. The desired trajectories x_{d_i} and $\dot{x}_{d_i}$ are once differentiable in time. Furthermore x_{d_i}, $\dot{x}_{d_i}$ and $\ddot{x}_{d_i}$ are available and with known bounds.

Assumption 3. The parameters $\bar{m}_i$ are unknown but positive and bounded, i.e., $0 < \bar{m}_{i\,\min} \le \bar{m}_i \le \bar{m}_{i\,\max}$.

Assumption 4. The components of $\bar{\mathbf{k}}$ and $\bar{\mathbf{h}}$ are unknown but bounded, i.e., $|\hat{\bar{k}}_i - \bar{k}_i| \le \kappa_i$ and $|\hat{\bar{h}}_i - \bar{h}_i| \le \zeta_i$.

Assumption 5. The components of $\bar{\mathbf{p}}$ are unknown but bounded, i.e., $|\bar{p}_i| \le \delta_i$.

Based on Assumption 3 and considering that the estimates $\hat{\hat{m}}_i$ could be chosen according to the geometric mean $\hat{\hat{m}}_i = \sqrt{\bar{m}_{i\,\max}\bar{m}_{i\,\min}}$, the bounds of $\bar{m}_i$ may be expressed as $\mu_i^{-1} \leq \hat{\hat{m}}_i/\bar{m}_i \leq \mu_i$, where $\mu_i = \sqrt{\bar{m}_{i\,\max}/\bar{m}_{i\,\min}}$.

Therefore, if we choose each control gain according to

$$K_i \geq \hat{\hat{m}}_i\mu_i\eta_i + \vartheta_i + |\hat{\hat{p}}_i| + \hat{\hat{m}}_i(\mu_i - 1)|\ddot{x}_{d_i} - \lambda_i\dot{\tilde{x}}_i| \tag{15}$$

where $\vartheta_i = \kappa_i + \zeta_i + \delta_i$ and each η_i is a strictly positive constant related to the reaching time, it can be easily verified that (13) is sufficient to impose the sliding condition

$$\frac{1}{2}\frac{\mathrm{d}}{\mathrm{d}t}s_i^2 \leq -\eta_i|s_i| \tag{16}$$

and, consequently, the finite time convergence to the sliding surface $S_i(t)$.

In order to obtain a good approximation to $\bar{\mathbf{p}}$, the estimates $\hat{\hat{p}}_i$ will be computed directly by an adaptive fuzzy algorithm.

The adopted fuzzy inference system is the zero-order TSK (Takagi–Sugeno–Kang), whose rules can be stated in a linguistic manner as follows:

If s_i is S_{i_r} then $\hat{\hat{p}}_{i_r} = \hat{P}_{i_r}$

where S_{i_r} are fuzzy sets, whose membership functions could be properly chosen, and $\hat{P}_{i_r}$ is the output value of each fuzzy rule r, with $r = 1, 2, \ldots, R$.

Considering that each rule defines a numerical value as output $\hat{P}_{i_r}$, the final output $\hat{\hat{p}}_i$ can be computed by a weighted average:

$$\hat{\hat{p}}_i(s_i) = \frac{\sum_{r=1}^{R} w_{i_r}\cdot\hat{P}_{i_r}}{\sum_{r=1}^{R} w_{i_r}} \tag{17}$$

or, similarly,

$$\hat{\hat{p}}_i(s_i) = \hat{\mathbf{P}}_i^{\mathrm{T}}\mathbf{\Psi}_i(s_i) \tag{18}$$

where, $\hat{\mathbf{P}}_i = [\hat{P}_{i_1}, \hat{P}_{i_2}, \ldots, \hat{P}_{i_R}]$ is the vector containing the attributed values $\hat{P}_{i_r}$ to each rule r, $\mathbf{\Psi}_i(s_i) = [\psi_{i_1}, \psi_{i_2}, \ldots, \psi_{i_R}]$ is a vector with components $\psi_{i_r}(s_i) = w_{i_r}/\sum_{r=1}^{R} w_{i_r}$ and w_{i_r} is the firing strength of each rule.

In order to obtain the most suitable values for $\hat{\hat{p}}_i(s_i)$, the vectors of adjustable parameters will be automatically updated by the following adaptation law:

$$\dot{\hat{\mathbf{P}}}_i = -\varphi_i s_i\mathbf{\Psi}_i(s_i) \tag{19}$$

where each φ_i is a strictly positive constant related to the adaptation rate.

It is important to emphasize that the chosen adaptation law, Eq. (19), must not only provide a good approximation to $\hat{\hat{p}}_i$ but also assure the convergence of the tracking variables to the sliding surface $S_i(t)$, for the purpose of trajectory tracking. In this way, in order to evaluate the convergence properties of the closed-loop system, let a positive-definite function V_i be defined as

$$V_i(t) = \frac{1}{2}s_i^2 + \frac{1}{2\mu_i\hat{\hat{m}}_i\varphi_i}\mathbf{\Delta}_i^{\mathrm{T}}\mathbf{\Delta}_i \tag{20}$$

where $\mathbf{\Delta}_i = \hat{\mathbf{P}}_i - \hat{\mathbf{P}}_i^*$ and $\hat{\mathbf{P}}_i^*$ is the optimal parameter vector, associated to the optimal estimate $\hat{\hat{p}}_i^*$. Thus, the time derivative of V_i is

$$\begin{aligned}\dot{V}_i(t) &= s_i\dot{s}_i + (\mu_i\hat{\hat{m}}_i\varphi_i)^{-1}\mathbf{\Delta}_i^{\mathrm{T}}\dot{\mathbf{\Delta}}_i\\ &= (\ddot{x}_i - \ddot{x}_{d_i} + \lambda_i\dot{\tilde{x}}_i)s_i + (\mu_i\hat{\hat{m}}_i\varphi_i)^{-1}\mathbf{\Delta}_i^{\mathrm{T}}\dot{\mathbf{\Delta}}_i\\ &= [\bar{m}_i^{-1}(\bar{\tau}_i - \bar{k}_i - \bar{h}_i - \bar{p}_i) - \ddot{x}_{d_i} + \lambda_i\dot{\tilde{x}}_i]s_i + (\mu_i\hat{\hat{m}}_i\varphi_i)^{-1}\mathbf{\Delta}_i^{\mathrm{T}}\dot{\mathbf{\Delta}}_i\end{aligned}$$

Defining a minimum approximation error as $\varepsilon_i = \hat{\hat{p}}_i^* - \bar{p}_i$ and noting that $\dot{\mathbf{\Delta}}_i = \dot{\hat{\mathbf{P}}}_i$ and $\mu_i^{-1} \leq \hat{\hat{m}}_i/\bar{m}_i \leq \mu_i$, then:

$$\begin{aligned}\dot{V}_i(t) \leq\; & -[K_i\,\mathrm{sgn}(s_i) - (\hat{\hat{k}}_i - \bar{k}_i) - (\hat{\hat{h}}_i - \bar{h}_i) - (\hat{\hat{p}}_i - \hat{\hat{p}}_i^*) - \varepsilon_i\\ & + \hat{\hat{m}}_i(\mu_i - 1)(\ddot{x}_{d_i} - \lambda_i\dot{\tilde{x}}_i)](\mu_i\hat{\hat{m}}_i)^{-1}s_i + (\mu_i\hat{\hat{m}}_i\varphi_i)^{-1}\mathbf{\Delta}_i^{\mathrm{T}}\dot{\hat{\mathbf{P}}}_i\\ =\; & -[K_i\,\mathrm{sgn}(s_i) - (\hat{\hat{k}}_i - \bar{k}_i) - (\hat{\hat{h}}_i - \bar{h}_i) - \mathbf{\Delta}_i^{\mathrm{T}}\mathbf{\Psi}_i(s_i) - \varepsilon_i\\ & + \hat{\hat{m}}_i(\mu_i - 1)(\ddot{x}_{d_i} - \lambda_i\dot{\tilde{x}}_i)](\mu_i\hat{\hat{m}}_i)^{-1}s_i + (\mu_i\hat{\hat{m}}_i\varphi_i)^{-1}\mathbf{\Delta}_i^{\mathrm{T}}\dot{\hat{\mathbf{P}}}_i\\ =\; & -[K_i\,\mathrm{sgn}(s_i) - (\hat{\hat{k}}_i - \bar{k}_i) - (\hat{\hat{h}}_i - \bar{h}_i) - \varepsilon_i + \hat{\hat{m}}_i(\mu_i - 1)(\ddot{x}_{d_i}\\ & - \lambda_i\dot{\tilde{x}}_i)](\mu_i\hat{\hat{m}}_i)^{-1}s_i + (\mu_i\hat{\hat{m}}_i\varphi_i)^{-1}\mathbf{\Delta}_i^{\mathrm{T}}[\dot{\hat{\mathbf{P}}}_i + \varphi_i s_i\mathbf{\Psi}_i(s_i)].\end{aligned}$$

By applying the adaptation law, Eq. (19), to $\dot{\hat{\mathbf{P}}}_i$, $\dot{V}_i(t)$ becomes:

$$\begin{aligned}\dot{V}_i(t) \leq\; & -[K_i\,\mathrm{sgn}(s_i) - (\hat{\hat{k}}_i - \bar{k}_i) - (\hat{\hat{h}}_i - \bar{h}_i) - \varepsilon_i\\ & + \hat{\hat{m}}_i(\mu_i - 1)(\ddot{x}_{d_i} - \lambda_i\dot{\tilde{x}}_i)](\mu_i\hat{\hat{m}}_i)^{-1}s_i.\end{aligned}$$

Furthermore, considering Assumptions 1–5, defining K_i according to (15) and verifying that $|\varepsilon_i| = |\hat{\hat{p}}_i^* - \bar{p}_i| \leq |\hat{\hat{p}}_i - \bar{p}_i| \leq |\hat{\hat{p}}_i| + \delta_i$, one has

$$\dot{V}_i(t) \leq -\eta_i|s_i| \tag{21}$$

which implies $V_i(t) \leq V_i(0)$ and that s_i and $\mathbf{\Delta}_i$ are bounded. Considering Assumption 2 and Eq. (12), it can be easily verified that $\dot{s}_i$ is also bounded.

Integrating both sides of (21) shows that

$$\lim_{t\to\infty}\int_0^t \eta_i|s_i|\mathrm{d}\theta \leq \lim_{t\to\infty}[V_i(0) - V_i(t)] \leq V_i(0) < \infty.$$

Since the absolute value function is uniformly continuous, it follows from Barbalat's lemma [46] that $s_i \to 0$ as $t \to \infty$, which ensures the convergence of the states to the sliding surface $S_i(t)$ and the desired trajectory tracking.

In spite of the demonstrated properties of the controller, the presence of a discontinuous term in the control law leads to the well known chattering phenomenon. To overcome the undesirable chattering effects, a thin boundary layer, S_{ϕ_i}, in the neighborhood of each switching surface can be adopted [13]:

$$S_{\phi_i} = \left\{(\tilde{x}_i, \dot{\tilde{x}}_i) \in \mathbb{R}^2 \mid |s_i(\tilde{x}_i, \dot{\tilde{x}}_i)| \leq \phi_i\right\}$$

where each ϕ_i is a strictly positive constant that represents the boundary layer thickness.

The boundary layer is achieved by replacing the sign function by a continuous interpolation inside S_{ϕ_i}. It should be noted that this smooth approximation must behave exactly like the sign function outside the boundary layer. There are several options to smooth out the ideal relay but the most common choice is the saturation function:

$$\mathrm{sat}(s_i/\phi_i) = \begin{cases}\mathrm{sgn}(s_i) & \text{if } |s_i/\phi_i| \geq 1\\ s_i/\phi_i & \text{if } |s_i/\phi_i| < 1.\end{cases}$$

In this way, to avoid chattering, a smooth version of Eq. (13) is defined:

$$\bar{\tau}_i = \hat{\hat{k}}_i + \hat{\hat{h}}_i + \hat{\hat{p}}_i + \hat{\hat{m}}_i\left(\ddot{x}_{d_i} - \lambda_i\dot{\tilde{x}}_i\right) - K_i\,\mathrm{sat}(s_i/\phi_i). \tag{22}$$

In order to establish the attractiveness and invariant properties of the defined boundary layer, let a new Lyapunov function candidate W_i be defined as

$$W_i(t) = \frac{1}{2}s_{\phi_i}^2 \tag{23}$$

where s_{ϕ_i} is a measure of the distance of the current state to the boundary layer, and can be computed as follows

$$s_{\phi_i} = s_i - \phi_i\,\mathrm{sat}(s_i/\phi_i). \tag{24}$$

Noting that $s_{\phi_i} = 0$ inside the boundary layer and $\dot{s}_{\phi_i} = \dot{s}_i$, one has $\dot{W}_i(t) = 0$ inside S_{ϕ_i}, and outside

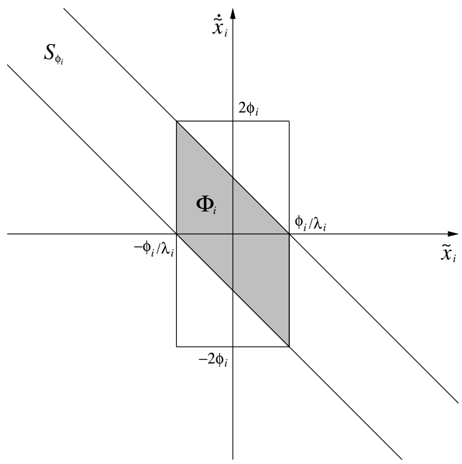

Fig. 2. Convergence region for the tracking error.

$$\dot{W}_i(t) = s_{\phi_i}\dot{s}_{\phi_i} = s_{\phi_i}\dot{s}_i = (\ddot{x}_i - \ddot{x}_{d_i} + \lambda_i\dot{\tilde{x}}_i)s_{\phi_i}$$
$$= [\bar{m}_i^{-1}(\bar{\tau}_i - \bar{k}_i - \bar{h}_i - \bar{p}_i) - \ddot{x}_{d_i} + \lambda_i\dot{\tilde{x}}_i]s_{\phi_i}.$$

It can be easily verified that outside the boundary layer the control law (22) takes the following form:

$$\bar{\tau}_i = \hat{\bar{k}}_i + \hat{\bar{h}}_i + \hat{\bar{p}}_i + \hat{\bar{m}}_i\left(\ddot{x}_{d_i} - \lambda_i\dot{\tilde{x}}_i\right) - K_i\,\mathrm{sgn}(s_{\phi_i}).$$

Thus, the time derivative $\dot{W}_i$ can be written as

$$\dot{W}_i(t) = -[K_i\,\mathrm{sgn}(s_{\phi_i}) - (\hat{\bar{k}}_i - \bar{k}_i) - (\hat{\bar{h}}_i - \bar{h}_i) - \hat{\bar{p}}_i + \bar{p}_i$$
$$- (\hat{\bar{m}}_i - \bar{m}_i)(\ddot{x}_{d_i} - \lambda_i\dot{\tilde{x}}_i)]\bar{m}_i^{-1}s_{\phi_i}.$$

So, considering Assumptions 1–5 and defining K_i according to (15), $\dot{W}_i(t)$ becomes:

$$\dot{W}_i(t) \le -\eta_i|s_{\phi_i}| \tag{25}$$

which implies $W_i(t) \le W_i(0)$ and that s_{ϕ_i} is bounded. From the definition of s_{ϕ_i}, Eq. (24), it can be easily verified that s_i is bounded. Considering Assumption 2 and Eq. (12), it can be concluded that $\dot{s}_i$ is also bounded.

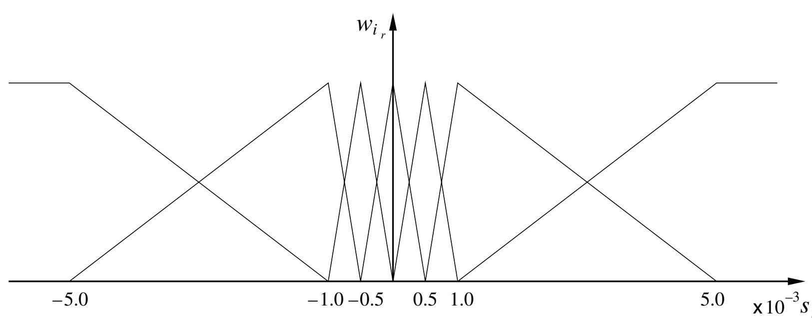

Fig. 3. Adopted fuzzy membership functions.

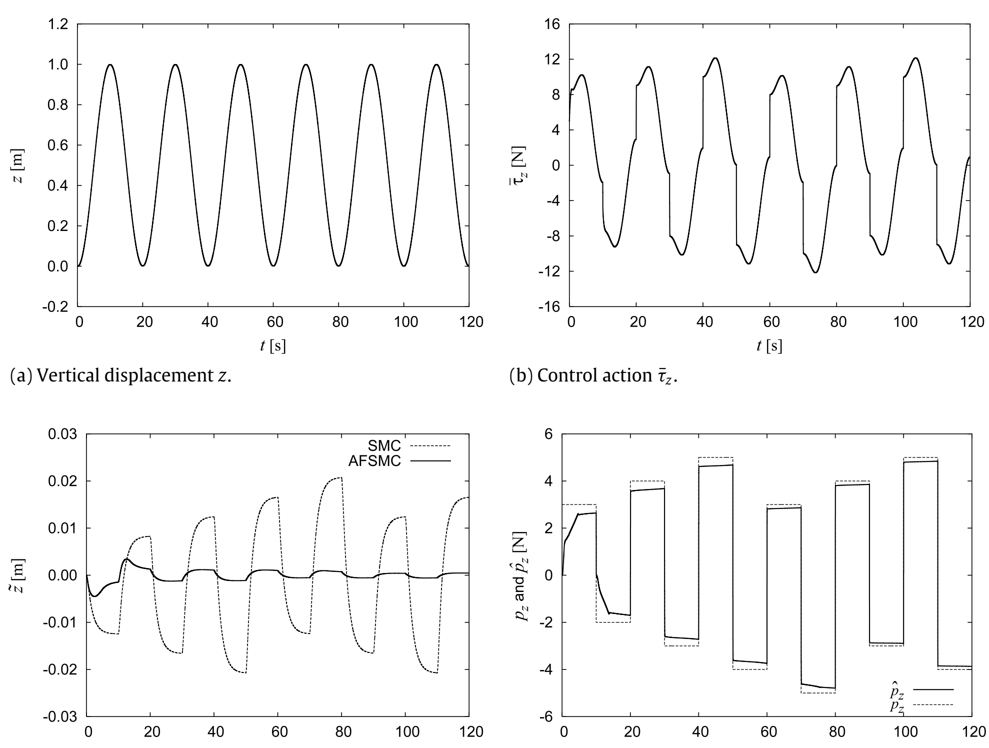

(a) Vertical displacement z.

(b) Control action $\bar{\tau}_z$.

(c) Tracking error $\tilde{z}$.

(d) Disturbance p_z and estimate $\hat{p}_z$.

Fig. 4. Depth control with known parameters and $\tilde{\mathbf{z}}(0) = \mathbf{0}$.

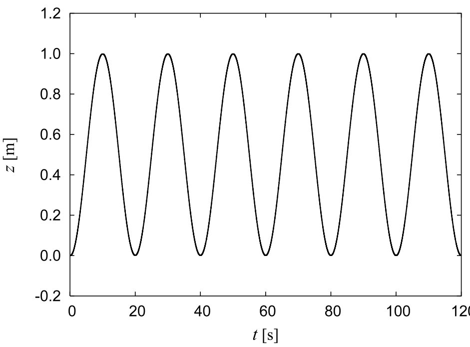

(a) Vertical displacement z.

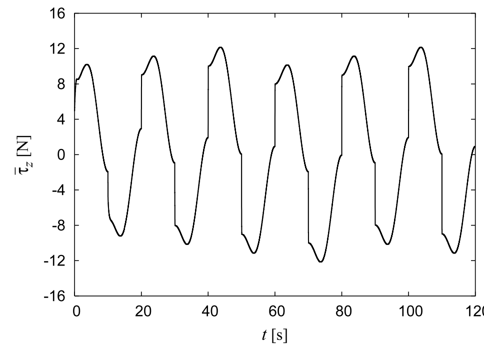

(b) Control action $\bar{\tau}_z$.

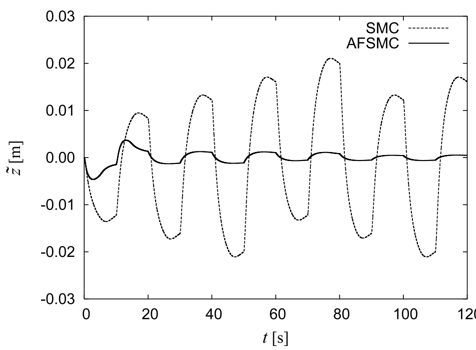

(c) Tracking error $\tilde{z}$.

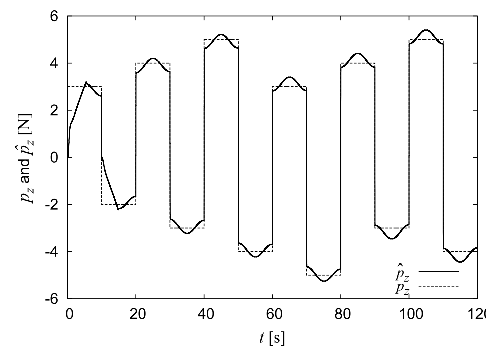

(d) Disturbance p_z and estimate $\hat{p}_z$.

Fig. 5. Depth control with uncertain parameters and $\tilde{\mathbf{z}}(0) = \mathbf{0}$.

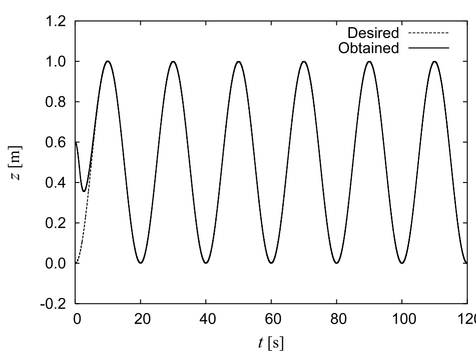

(a) Vertical displacement z.

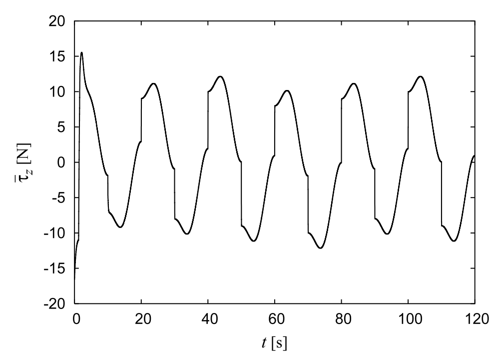

(b) Control variable u.

Fig. 6. Tracking with uncertain parameters and $\tilde{\mathbf{z}}(0) = [0.6, 0.0]$.

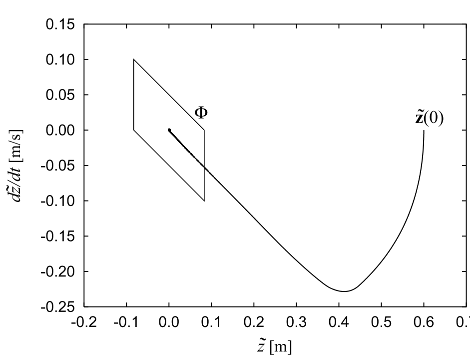

(a) With the proposed AFSMC.

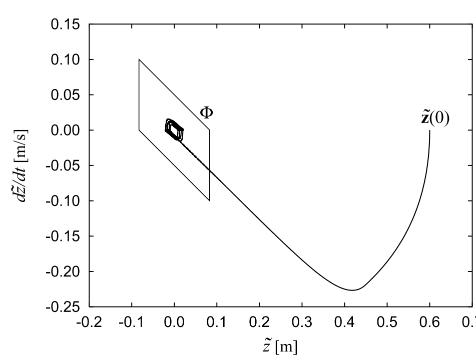

(b) With the conventional SMC.

Fig. 7. Phase portrait of the trajectory tracking with $\tilde{\mathbf{z}}(0) = [0.6, 0.0]$.

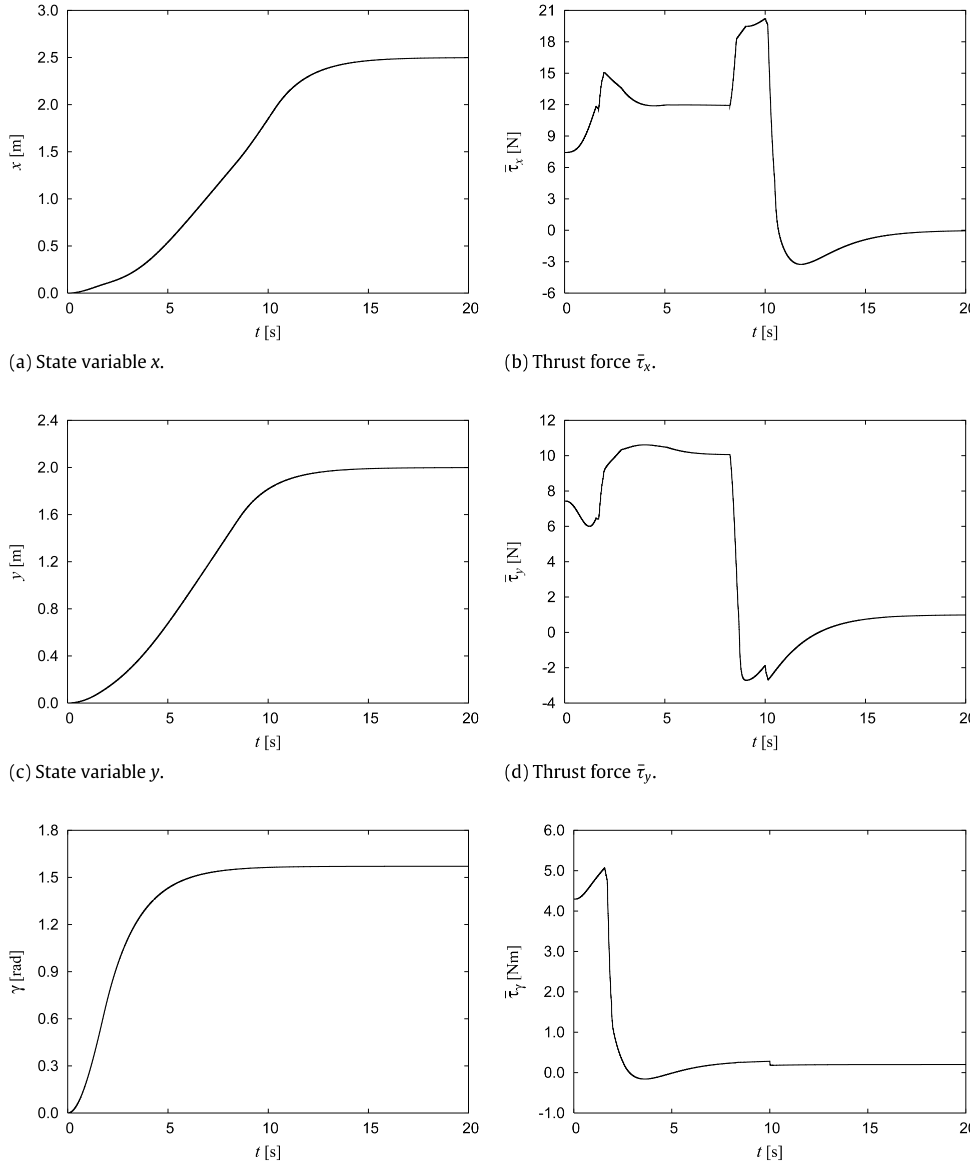

(a) State variable x.

(b) Thrust force $\bar{\tau}_x$.

(c) State variable y.

(d) Thrust force $\bar{\tau}_y$.

(e) State variable γ.

(f) Thrust force $\bar{\tau}_\gamma$.

Fig. 8. Dynamic positioning in the plane XY.

The finite time convergence of the states to the boundary layer can be shown by integrating both sides of (25) over the interval $0 \le t \le t_{\text{reach}_i}$, where t_{reach_i} is the time required to hit S_{ϕ_i}. In this way, noting that $|s_{\phi_i}(t_{\text{reach}_i})| = 0$, one has:

$$t_{\text{reach}_i} \le \frac{|s_{\phi_i}(0)|}{\eta_i} \tag{26}$$

which guarantees the convergence of the tracking error vector to the boundary layer in a time interval smaller than $|s_{\phi_i}(0)|/\eta_i$.

Nevertheless, it should be emphasized that the substitution of the discontinuous term by a smooth approximation inside the boundary layer turns the perfect tracking into a tracking with guaranteed precision problem, which actually means that a steady-state error will always remain. However, it can be easily verified that, once inside the boundary layer, the tracking error vector will exponentially converge to a closed region Φ_i.

Considering that $|s_i(\tilde{x}_i, \dot{\tilde{x}}_i)| \le \phi_i$ may be rewritten as $-\phi_i \le s_i(\tilde{x}_i, \dot{\tilde{x}}_i) \le \phi_i$ and from the definition of $s_i(\tilde{x}_i, \dot{\tilde{x}}_i)$, Eq. (12), one has:

$$-\phi_i \le \dot{\tilde{x}}_i + \lambda_i \tilde{x}_i \le \phi_i. \tag{27}$$

Thus, multiplying (27) by $e^{\lambda_i t}$ and integrating between 0 and t:

$$-\phi_i e^{\lambda_i t} \le (\dot{\tilde{x}}_i + \lambda_i \tilde{x}_i) e^{\lambda_i t} \le \phi_i e^{\lambda_i t}$$

$$-\phi_i e^{\lambda_i t} \le \frac{d}{dt}(\tilde{x}_i e^{\lambda_i t}) \le \phi_i e^{\lambda_i t}$$

$$-\phi_i \int_0^t e^{\lambda_i \theta} d\theta \le \int_0^t \frac{d}{d\tau}(\tilde{x}_i e^{\lambda_i \theta}) d\theta \le \phi_i \int_0^t e^{\lambda_i \theta} d\theta$$

$$-\frac{\phi_i}{\lambda_i} e^{\lambda_i t} + \frac{\phi_i}{\lambda_i} \le \tilde{x}_i(t) e^{\lambda_i t} - \tilde{x}_i(0) \le \frac{\phi_i}{\lambda_i} e^{\lambda_i t} - \frac{\phi_i}{\lambda_i}$$

$$-\frac{\phi_i}{\lambda_i} - \left[|\tilde{x}_i(0)| + \frac{\phi_i}{\lambda_i}\right] e^{-\lambda_i t} \le \tilde{x}_i(t) \le \frac{\phi_i}{\lambda_i} + \left[|\tilde{x}_i(0)| + \frac{\phi_i}{\lambda_i}\right] e^{-\lambda_i t}.$$

Furthermore, for $t \to \infty$:

$$-\frac{\phi_i}{\lambda_i} \le \tilde{x}_i \le \frac{\phi_i}{\lambda_i}. \tag{28}$$

By applying (28) to (27), it can be easily verified that:

$$-2\phi_i \le \dot{\tilde{x}}_i \le 2\phi_i. \tag{29}$$

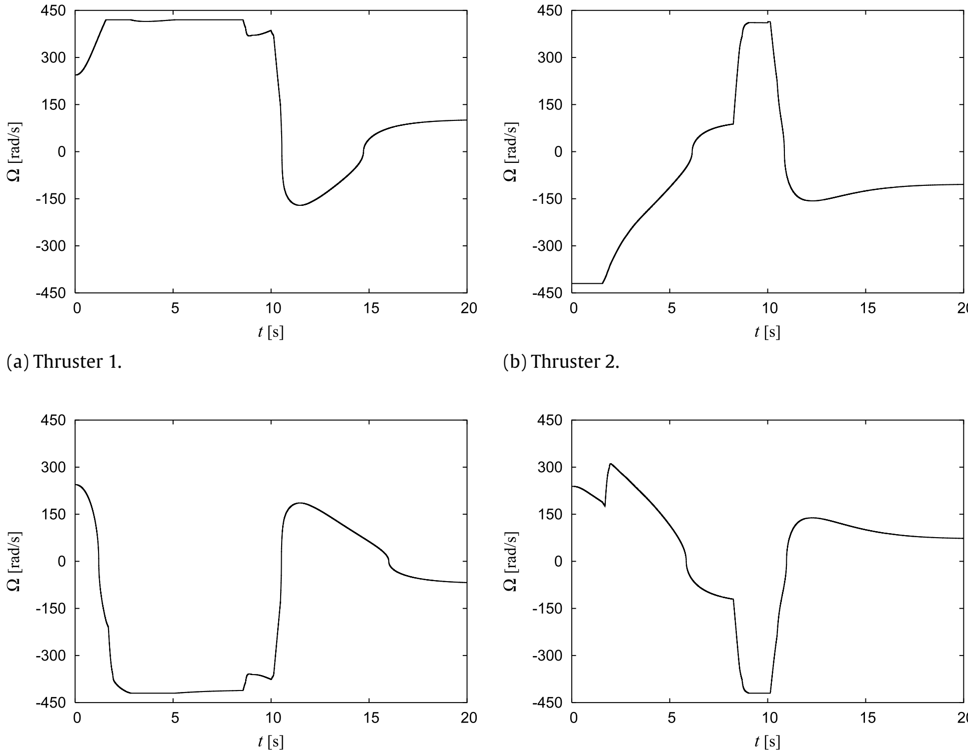

(a) Thruster 1.

(b) Thruster 2.

(c) Thruster 3.

(d) Thruster 4.

Fig. 9. Propeller's angular velocity related to the dynamic positioning in the plane XY.

In this way, the tracking error will be confined within the limits $|\tilde{x}_i| \leq \phi_i/\lambda_i$ and $|\dot{\tilde{x}}_i| \leq 2\phi_i$. However, these bounds define a box that is not completely inside the boundary layer, as can be seen in Fig. 2.

Considering the demonstrated attractiveness and invariant properties of S_{ϕ_i}, the region of convergence can be stated as the intersection of the boundary layer and the box defined by the preceding bounds. Therefore, it follows that the tracking error vector will exponentially converge to a closed region $\Phi_i = \{(\tilde{x}_i, \dot{\tilde{x}}_i) \in \mathbb{R}^2 \mid |s_i(\tilde{x}_i, \dot{\tilde{x}}_i)| \leq \phi_i \text{ and } |\tilde{x}_i| \leq \lambda_i^{-1}\phi_i \text{ and } |\dot{\tilde{x}}_i| \leq 2\phi_i\}$. This result proves that the convergence region of the tracking error vector is even smaller than that shown in [3] and is in perfect accordance with the bounds proposed by Bessa [47] for nth-order nonlinear systems subject to smooth sliding mode controllers.

4. Simulation results

The numerical simulations were carried out considering the fourth-order Runge–Kutta method and sampling rates of 500 Hz for the control system and 1 kHz for the dynamic model. The chosen parameters for the ROV model were $\mathbf{M} = \text{diag}\{80 \text{ kg}, 80 \text{ kg}, 100 \text{ kg}, 8 \text{ kg m}^2\}$ and $\mathbf{h} = [125\,\upsilon_x|\upsilon_x| \text{ N}, 175\upsilon_y|\upsilon_y| \text{ N}, 250\upsilon_z|\upsilon_z| \text{ N}, 12.5\omega_z|\omega_z| \text{ N m}]$. Considering that electrically actuated bladed thrusters are the most common choices to equip underwater vehicles and that the propeller's angular velocity of these thrusters is limited, due to the maximal current/voltage admitted by the thruster's DC motors, a saturation limited angular velocity, with $\Omega_{\max} = 420$ rad/s and $C_T = 4.5 \times 10^{-5}$, was adopted for Eq. (5). The disturbance forces and moments were chosen to vary in the range of ± 5 N and ± 0.5 N m, respectively.

Concerning the fuzzy system, the same triangular and trapezoidal membership functions, with the central values defined as $C_i = \{-5.0; -1.0; -0.5; 0.0; 0.5; 1.0; 5.0\} \times 10^{-3}$ (see Fig. 3), were adopted for each DOF. The vectors of adjustable parameters were initialized to zero, $\hat{\mathbf{D}}_i = \mathbf{0}$, and automatically updated at each iteration step according to the adaptation law, Eq. (19).

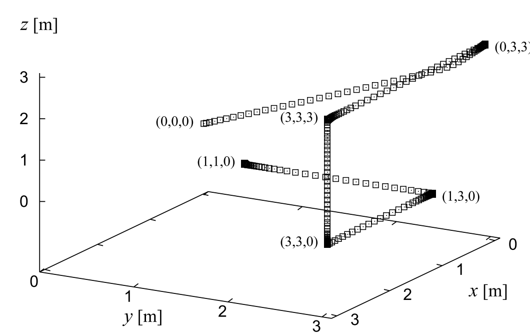

Fig. 10. Dynamic positioning in $\mathbb{R}^3$.

To evaluate the control system performance, five different numerical simulations were performed. The obtained results are presented in Figs. 4–11.

In the first case, it was assumed that the model parameters were perfectly known, i.e., the estimates of $\mathbf{M}$ and $\mathbf{h}$ were defined as $\hat{\mathbf{M}} = \mathbf{M}$ and $\hat{\mathbf{h}} = \mathbf{h}$ in the control law. In order to simplify the design process, the other controller parameters were chosen identical for all degrees of freedom, $\phi_i = 0.05$, $\eta_i = 0.1$, $\lambda_i = 0.6$, $\mu_i = 1.1$, $\vartheta_i = 10$ and $\varphi_i = 500$. Fig. 4 gives the corresponding results for the tracking of $z_d = 0.5[1 - \cos(0.1\pi t)]$.

As observed in Fig. 4, even in the presence of external disturbances, the adaptive fuzzy sliding mode controller (AFSMC) is capable to provide the trajectory tracking with a small associated error and no chattering at all. It can be also verified that the proposed control law provides a smaller tracking error when compared with the conventional sliding mode controller (SMC), Fig. 4(c). The improved performance of AFSMC over SMC is due to its ability to recognize and compensate the external disturbances,

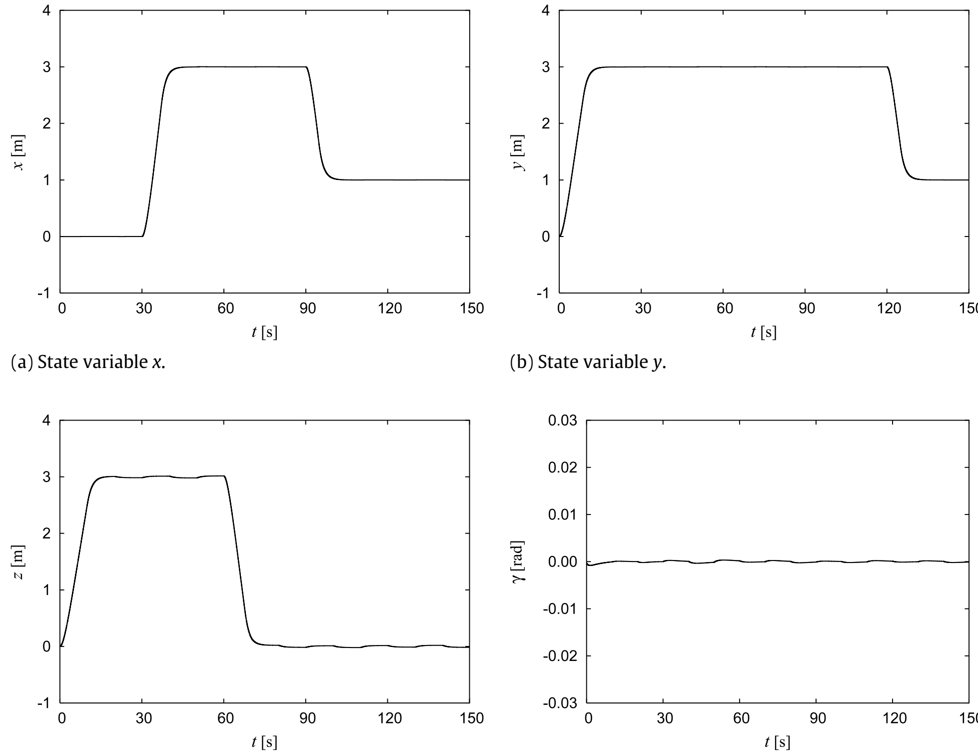

(a) State variable x.

(b) State variable y.

(c) State variable z.

(d) State variable γ.

Fig. 11. State variables in the time domain related to the dynamic positioning in $\mathbb{R}^3$.

Fig. 4(d). The AFSMC can be easily converted to the classical SMC by setting the adaptation rate to zero, $\varphi_i = 0$.

It should be also noted that, since $\hat{\hat{p}}_i$ is based on the universal approximation feature of a fuzzy inference system [48], and not just an ordinary adaptive parameter, it represents disturbances and uncertainties as functions of s_i. On this basis, it provides faster accommodation to disturbance variations than would be obtained using a simple adaptive parameter.

In the next four simulation studies, the parameters for the controller were chosen based on the assumption that exact values are not known but with a maximal uncertainty of $\pm 10\%$ over previous adopted values, $\hat{\mathbf{M}} = \text{diag}\{79.5\text{ kg}, 79.5\text{ kg}, 99.5\text{ kg}, 7.9\text{ kgm}^2\}$ and $\hat{\mathbf{h}} = [112.5\upsilon_x|\upsilon_x|\text{ N}, 157.5\upsilon_y|\upsilon_y|\text{N}, 225\upsilon_z|\upsilon_z|\text{N}, 11.3\omega_z|\omega_z|\text{N m}]$. The other parameters, as well as the disturbance force, were defined as before. Fig. 5 shows the results obtained for the tracking of $z_d = 0.5[1 - \cos(0.1\pi t)]$.

Despite the external disturbance forces and uncertainties with respect to model parameters, the AFSMC allows the remotely operated underwater vehicle to track the desired trajectory with a small tracking error (see Fig. 5). As before, the undesirable chattering effect was not observed, Fig. 5(b). Through the comparative analysis showed in Fig. 5(c), the improved performance of the AFSMC over the uncompensated counterpart can be clearly ascertained.

In the third simulation the initial state and initial desired state are not equal, $\tilde{\mathbf{z}}(0) = [0.6, 0.0]$. Figs. 6 and 7 show the corresponding results. The phase portrait related to the tracking obtained with the proposed control scheme is shown in Fig. 7(a). For comparison purposes, the phase portrait obtained with the conventional sliding modes is also presented, Fig. 7(b). Note that in both situations the steady-state tracking error remains on the convergence region Φ, but the improved performance of the AFSMC can be easily observed.

Now, considering the motion in the XY plane, the underwater vehicle was intended to move from its initial position/orientation at rest, $\mathbf{x}_0 = [0, 0, 0, 0]$, to the desired final position/orientation $\mathbf{x}_d = [2.5, 2, 0, \pi/2]$. Once this final position/orientation is reached, it should stay there indefinitely, besides the disturbance forces. The obtained results are presented in Figs. 8 and 9.

Fig. 8 shows the obtained response in the time domain. These results confirm that the proposed control strategy was able to regulate and stabilize the dynamical behavior of the underwater vehicle in the horizontal plane. As observed in Fig. 8(b), (d) and (f), the adaptive fuzzy sliding mode controller was also efficient in minimizing the undesirable chattering effect. The propeller's angular velocity, associated to the control problem in the horizontal plane, are presented in Fig. 9.

Finally, the last simulation study was a trajectory tracking in $\mathbb{R}^3$. Here, from the initial position $\mathbf{x}_0 = [0, 0, 0, 0]$ at rest, the vehicle was forced to move to the following desired positions: $\mathbf{x}_1 = [0, 3, 3, 0]$, $\mathbf{x}_2 = [3, 3, 3, 0]$, $\mathbf{x}_3 = [3, 3, 0, 0]$, $\mathbf{x}_4 = [1, 3, 0, 0]$ and $\mathbf{x}_5 = [1, 1, 0, 0]$, where $t_0 = 0$ s, $t_1 = 30$ s, $t_2 = 60$ s, $t_3 = 90$ s, $t_4 = 120$ s, $t_5 = 150$ s. During the entire path, the yaw angle should be kept constant, $\gamma = 0$. The obtained results are presented in Figs. 10 and 11.

By observing both figures, it can be verified that, with the proposed control system, the vehicle could follow the desired trajectory, in spite of the disturbance forces. It can be also observed, Fig. 11(d), that the yaw angle (γ) was held within the acceptable bounds, defined by the chosen width of the boundary layer, $\phi_\gamma = 0.05$.

5. Concluding remarks

In this paper, the problem of compensating uncertainty/disturbance in the dynamic positioning system of remotely operated underwater vehicles was considered. An adaptive fuzzy sliding mode controller was implemented to deal with the stabilization and trajectory tracking problems. The adoption of a reduced order mathematical model for the underwater vehicle and the development of a control system in a decentralized fashion, neglecting cross-coupling terms, was discussed. The boundedness and convergence properties of the closed-loop system were analytically proven using Lyapunov stability theory and Barbalat's lemma. By means of numerical simulations, it could be verified that the proposed strategy was able to cope with both the disturbances, that can typically arise in the subaquatic environment, and uncertainties in hydrodynamics coefficients. As observed, the incorporation of an adaptive fuzzy algorithm within the boundary layer made a better trade-off between tracking performance and chattering possible.

Acknowledgement

The authors acknowledge the support of the State of Rio de Janeiro Research Foundation (FAPERJ).

References

[1] J. Yuh, Learning control for underwater robotic vehicles, IEEE Control Systems Magazine 14 (2) (1994) 39–46.
[2] K.R. Goheen, E.R. Jeffreys, Multivariable self-tuning autopilots for autonomous and remotely operated underwater vehicles, IEEE Journal of Oceanic Engineering 15 (3) (1990) 144–151.
[3] W.M. Bessa, M.S. Dutra, E. Kreuzer, Depth control of remotely operated underwater vehicles using an adaptive fuzzy sliding mode controller, Robotics and Autonomous Systems 56 (8) (2008) 670–677.
[4] N.Q. Hoang, E. Kreuzer, A robust adaptive sliding mode controller for remotely operated vehicles, Technische Mechanik 28 (3–4) (2008) 185–193.
[5] E. Sebastián, M.A. Sotelo, Adaptive fuzzy sliding mode controller for the kinematic variables of an underwater vehicle, Journal of Intelligent and Robotic Systems 49 (2) (2007) 189–215.
[6] T. Chatchanayuenyong, M. Parnichkun, Neural network based-time optimal sliding mode control for an autonomous underwater robot, Mechatronics 16 (8) (2007) 471–478.
[7] A. Pisano, E. Usai, Output-feedback control of an underwater vehicle prototype by higher-order sliding modes, Automatica 40 (9) (2004) 1525–1531.
[8] J. Guo, F.C. Chiu, C.C. Huang, Design of a sliding mode fuzzy controller for the guidance and control of an autonomous underwater vehicle, Ocean Engineering 30 (16) (2003) 2137–2155.
[9] E. Kreuzer, F.C. Pinto, Controlling the position of a remotely operated underwater vehicle, Applied Mathematics and Computation 78 (2–3) (1996) 175–185.
[10] R. Christi, F.A. Papoulias, A.J. Healey, Adaptive sliding mode control of autonomous underwater vehicles in dive plane, IEEE Journal of Oceanic Engineering 15 (3) (1990) 152–160.
[11] A.J. Healey, D. Lienard, Multivariable sliding mode control for autonomous diving and steering of unmanned underwater vehicles, IEEE Journal of Oceanic Engineering 18 (3) (1993) 327–339.
[12] D.R. Yoerger, J.-J.E. Slotine, Robust trajectory control of underwater vehicles, IEEE Journal of Oceanic Engineering 10 (4) (1985) 462–470.
[13] J.-J.E. Slotine, Sliding controller design for nonlinear systems, International Journal of Control 40 (2) (1984) 421–434.
[14] L.-X. Wang, Stable adaptive fuzzy control of nonlinear systems, IEEE Transactions on Fuzzy Systems 1 (2) (1993) 146–155.
[15] R. Palm, Robust control by fuzzy sliding mode, Automatica 30 (9) (1994) 1429–1437.
[16] T. Chai, S. Tong, Fuzzy direct adaptive control for a class of nonlinear systems, Fuzzy Sets and Systems 103 (3) (1999) 379–387.
[17] R.G. Berstecher, R. Palm, H.D. Unbehauen, An adaptive fuzzy sliding-mode controller, IEEE Transactions on Industrial Electronics 48 (1) (2001) 18–31.
[18] L.K. Wong, F.H.F. Leung, P.K.S. Tam, A fuzzy sliding controller for nonlinear systems, IEEE Transactions on Industrial Electronics 48 (1) (2001) 32–37.
[19] Q.P. Ha, Q.H. Nguyen, D.C. Rye, H.F. Durrant-Whyte, Fuzzy sliding mode controllers with applications, IEEE Transactions on Industrial Electronics 48 (1) (2001) 38–46.
[20] C.-Y. Liang, J.-P. Su, A new approach to the design of a fuzzy sliding mode controller, Fuzzy Sets and Systems 139 (1) (2003) 111–124.
[21] C.-C. Cheng, S.-H. Chien, Adaptive sliding mode controller design based on T–S fuzzy system model, Automatica 42 (6) (2006) 1005–1010.
[22] T.-Z. Wu, Y.-T. Juang, Adaptive fuzzy sliding-mode controller of uncertain nonlinear systems, ISA Transactions 47 (3) (2008) 279–285.
[23] B. Yoo, W. Ham, Adaptive fuzzy sliding mode control of nonlinear system, IEEE Transactions on Fuzzy Systems 6 (2) (1998) 315–321.
[24] J.-P. Su, T.-M. Chen, C.-C. Wang, Adaptive fuzzy sliding mode control with GA-based reaching laws, Fuzzy Sets and Systems 120 (1) (2001) 145–158.
[25] J. Wang, A.B. Rad, P.T. Chan, Indirect adaptive fuzzy sliding mode control: Part I: Fuzzy switching, Fuzzy Sets and Systems 122 (1) (2001) 21–30.
[26] J. Wang, A.B. Rad, P.T. Chan, Indirect adaptive fuzzy sliding mode control: Part II: Parameter projection and supervisory control, Fuzzy Sets and Systems 122 (1) (2001) 31–43.
[27] W. Chang, J.B. Park, Y.H. Joo, G. Chen, Design of robust fuzzy-model-based controller with sliding mode control for SISO nonlinear systems, Fuzzy Sets and Systems 125 (1) (2002) 1–22.
[28] C.-C. Kung, T.-H. Chen, Observer-based indirect adaptive fuzzy sliding mode control with state variable filters for unknown nonlinear dynamical systems, Fuzzy Sets and Systems 155 (2) (2005) 292–308.
[29] W.M. Bessa, R.S.S. Barrêto, Adaptive fuzzy sliding mode control of uncertain nonlinear systems, Controle & Automação, (2009)(in press).
[30] W.M. Bessa, A.S. De Paula, M.A. Savi, Chaos control using an adaptive fuzzy sliding mode controller with application to a nonlinear pendulum, Chaos, Solitons & Fractals 42 (2) (2009) 784–791.
[31] G. Antonelli, On the use of adaptive/integral actions for six-degrees-of-freedom control of autonomous underwater vehicles, IEEE Journal of Oceanic Engineering 32 (2) (2007) 300–312.
[32] N.Q. Hoang, E. Kreuzer, Adaptive PD-controller for positioning of a remotely operated vehicle close to an underwater structure: Theory and experiments, Control Engineering Practice 15 (4) (2007) 411–419.
[33] D.A. Smallwood, L.L. Whitcomb, Model-based dynamic positioning of underwater robotic vehicles: Theory and experiment, IEEE Journal of Oceanic Engineering 29 (1) (2004) 169–186.
[34] L. Hsu, R.R. Costa, F. Lizarralde, J.P.V.S. Da Cunha, Dynamic positioning of remotely operated underwater vehicles, IEEE Robotics and Automation Magazine 7 (3) (2000) 21–31.
[35] P. Kiriazov, E. Kreuzer, F.C. Pinto, Robust feedback stabilization of underwater robotic vehicles, Robotics and Autonomous Systems 21 (4) (1997) 415–423.
[36] S.M. Zanoli, G. Conte, Remotely operated vehicle depth control, Control Engineering Practice 11 (4) (2003) 453–459.
[37] F.C. Pinto, Theoretische und experimentelle Untersuchung zur Sensorik und Regelung von Unterwasserfahrzeugen, VDI Verlag, Düsseldorf, 1996.
[38] J.P.V.S. Da Cunha, R.R. Costa, L. Hsu, Design of a high performance variable structure control of ROVs, IEEE Journal of Oceanic Engineering 20 (1) (1995) 42–55.
[39] L. Bevilacqua, W. Kleczca, E. Kreuzer, On the mathematical modeling of ROVs, in: I. Troch, K. Desoyer, P. Kopacek (Eds.), Proceedings of the Symposium on Robot Control, Vienna, Austria, 1991, pp. 595–598.
[40] J.N. Newman, Marine Hydrodynamics, 5th edition, MIT Press, MA, 1986.
[41] W. Kleczka, E. Kreuzer, F.C. Pinto, Analytic–numeric study of a submerged double pendulum, in M.P. Paidoussis, M.K. Au-Yang (Eds.), International Symposium on Flow-Induced Vibration and Noise, Anaheim, USA, 1992.
[42] D.A. Smallwood, L.L. Whitcomb, Adaptive identification of dynamically positioned underwater robotic vehicles, IEEE Transactions on Control Systems Technology 11 (4) (2003) 505–515.
[43] R. Bachmayer, L.L. Whitcomb, M.A. Grosenbaugh, An accurate four-quadrant nonlinear dynamical model for marine thrusters: Theory & experimental validation, IEEE Journal of Oceanic Engineering 25 (1) (2000) 146–159.
[44] L.L. Whitcomb, D.R. Yoerger, Development, comparison, and preliminary experimental validation of non-linear dynamic thruster models, IEEE Journal of Oceanic Engineering 24 (4) (1999) 481–494.
[45] J.-J.E. Slotine, Tracking control of nonlinear systems using sliding surfaces, Ph.D. Thesis, Massachusetts Institute of Technology, Cambridge, 1983.
[46] H.K. Khalil, Nonlinear Systems, 3rd edition, Prentice Hall, NJ, 2001.
[47] W.M. Bessa, Some remarks on the boundedness and convergence properties of smooth sliding mode controllers, International Journal of Automation and Computing 6 (2) (2009) 154–158.
[48] B. Kosko, Fuzzy systems as universal approximators, IEEE Transactions on Computers 43 (11) (1994) 1329–1333.

Wallace M. Bessa was born in Rio de Janeiro, Brazil in 1975. He earned the B.Sc. degree from the State University of Rio de Janeiro, Brazil, in 1997, the M.Sc. degree at the Military Institute of Engineering, Rio de Janeiro, Brazil, in 2000 and the D.Sc. degree at the Federal University of Rio de Janeiro, Brazil, in 2005, all in Mechanical Engineering. Part of his doctoral research was developed at the Institute for Mechanical and Ocean Engineering of the Hamburg University of Technology, from 2002 to 2003. He is currently Associate Professor at the Federal University of Rio Grande do Norte, Brazil. His research interests include robotics, control theory, fuzzy logic and nonlinear dynamics. He is member of the International Physics and Control Society (IPACS), American Mathematical Society (AMS), Brazilian Mathematical Society (Sociedade Brasileira de Matemática, SBM), Brazilian Society for Applied and Computational Mathematics (Sociedade Brasileira de Matemática Aplicada e Computacional, SBMAC) and Brazilian Association for Mechanical Engineering and Sciences (Associação Brasileira de Engenharia e Ciências Mecânicas, ABCM).

Max S. Dutra earned the B.Sc. degree in Mechanical Engineering from the Fluminense Federal University, Niterói, Brazil, in 1987, the M.Sc. degree in Mechanical Engineering at the Federal University of Rio de Janeiro, Brazil, in 1990 and the Dr.-Ing. degree from the Gerhard Mercator University, Duisburg, Germany, in 1995. From 1997 to 1995 he was Assistant Professor at the Paulista State University, Ilha Solteira, Brazil and since 1999 he is Associate Professor at the Federal University of Rio de Janeiro. His research interests include nonlinear dynamics and control, robotics, mechatronics and flexible manufacturing systems. He is member of the Brazilian Association for Mechanical Engineering and Sciences (Associação Brasileira de Engenharia e Ciências Mecânicas, ABCM).

Edwin Kreuzer began his university studies at the Technical University of Munich, Germany. There he earned the diploma degree (Dipl.-Ing.) in Mechanical Engineering. He earned his doctoral degree (Dr.-Ing.) and habilitation (Dr.-Ing. habil.) from the University of Stuttgart, Germany. He was an Assistant Professor and Professor at the University of Stuttgart. Subsequently he went to the Hamburg University of Technology, Hamburg. There he is head of the Institute of Mechanics and Ocean Engineering since 1996. Since April 2005 he is President of the Hamburg University of Technology. Professor Kreuzer has been a Visiting Scholar and Visiting Professor at the University of California at Berkeley, USA, and a Visiting Professor at the Federal University of Rio de Janeiro, Brazil. At the University of California at Berkeley he was awarded the Russel Severance Springer Guest-Professorship of the Department of Mechanical Engineering. He is Honorary Professor of Nanjing University of Science and Technology. He has presented invited lectures all over the world. He has more than 200 publications on topics such as multibody system dynamics, active mechanical systems, structural dynamics, nonlinear dynamics, dynamic stability, and ocean engineering. He has published four books and contributed chapters to several others. He was co-editor-in-chief of the Journal of Applied Mathematics and Mechanics (Zeitschrift für Angewandte Mathematik and Mechanik ZAMM) 1996–2005, co-editor of the book series Advances in Engineering and he is member of the editorial board of three other international journals. He is member of the Academy of Sciences, Hamburg, as well as member of several research societies and served as Secretary General of the Society of Applied Mathematics and Mechanics (Gesellschaft für Angewandte Mathematik und Mechanik, GAMM).